学位論文

Tumor metabolic alterations after neoadjuvant chemoradiotherapy predict postoperative recurrence in patients with pancreatic cancer

香川大学医学部医学系研究科
医学専攻

和田　侑希子

JJCO Japanese Journal of Clinical Oncology

Japanese Journal of Clinical Oncology, 2022, 1–10
https://doi.org/10.1093/jjco/hyac074
Original Article

OXFORD

Original Article

Tumor metabolic alterations after neoadjuvant chemoradiotherapy predict postoperative recurrence in patients with pancreatic cancer

Yukiko Wada[1], Keiichi Okano[1,*], Kiyotoshi Sato[2], Masahiro Sugimoto[2], Ayaka Shimomura[1], Mina Nagao[1], Hiroyuki Matsukawa[1], Yasuhisa Ando[1], Hironobu Suto[1], Minoru Oshima[1], Akihiro Kondo[1], Eisuke Asano[1], Takayoshi Kishino[1], Kensuke Kumamoto[1], Hideki Kobara[3], Hideki Kamada[3], Tsutomu Masaki[3], Tomoyoshi Soga[2], and Yasuyuki Suzuki[1]

[1]Department of Gastroenterological Surgery, Kagawa University, Kita-gun, Kagawa, Japan, [2]Institute for Advanced Biosciences, Keio University, Kakuganji, Tsuruoka, Japan, and [3]Department of Gastroenterology and Neurology, Kagawa University, Takamatsu, Kagawa, Japan

*For reprints and all correspondence: Keiichi Okano, Department of Gastroenterological Surgery, Faculty of Medicine, Kagawa University, 1750-1 Ikenobe, Miki-cho, Kita-gun, Kagawa 761-0793, Japan. E-mail: okano.keiichi@kagawa-u.ac.jp

Received 9 December 2021; Editorial Decision 9 April 2022; Accepted 13 April 2022

Abstract

Objective: We investigated the metabolic changes in pancreatic ductal adenocarcinoma to identify the mechanisms of treatment response of neoadjuvant chemoradiation therapy.

Methods: Frozen tumor and non-neoplastic pancreas tissues were prospectively obtained from 88 patients with pancreatic ductal adenocarcinoma who underwent curative-intent surgery. Sixty-two patients received neoadjuvant chemoradiation therapy and 26 patients did not receive neoadjuvant therapy (control group). Comprehensive analysis of metabolites in tumor and non-neoplastic pancreatic tissue was performed by capillary electrophoresis-mass spectrometry.

Results: Capillary electrophoresis-mass spectrometry detected 90 metabolites for analysis among more than 500 ionic metabolites quantified. There were significant differences in 27 tumor metabolites between the neoadjuvant chemoradiation therapy and control groups. There were significant differences in eight metabolites [1-MethylnNicotinamide, Carnitine, Glucose, Glutathione (red), N-acetylglucosamine 6-phosphate, N-acetylglucosamine 1-phosphate, UMP, Phosphocholine] between good responder and poor responder for neoadjuvant chemoradiation therapy. Among these metabolites, phosphocholine, Carnitine and Glutathione were associated with recurrence-free survival only in the neoadjuvant chemoradiation therapy group. Microarray confirmed marked gene suppression of choline transporters [CTL1-4 (SLC44A1-44A4)] in pancreatic ductal adenocarcinoma tissue of neoadjuvant chemoradiation therapy group.

Conclusion: The present study identifies several important metabolic consequences and potential neoadjuvant chemoradiation therapy targets in pancreatic ductal adenocarcinoma. Choline metabolism is one of the key pathways involved in recurrence of the patients with pancreatic ductal adenocarcinoma who received neoadjuvant chemoradiation therapy.

Key words: metabolomics, neoadjuvant therapy, PDAC, choline, CE-MS

Introduction

The efficacy of postoperative adjuvant therapy for pancreatic ductal adenocarcinoma (PDAC) has been proven (1). Recently, the effect of preoperative chemotherapies has been reported (2), and neoadjuvant therapy of gemcitabine plus S-1 became a standard treatment for resectable PDAC. We executed a phase II trial of preoperative short-term chemoradiation therapy for resectable and borderline resectable pancreatic cancer (3). The study confirmed that the protocol allowed high rates of treatment completion (91%) and subsequent resection (96%) with pathologically negative margins (98%). On the other hand, a certain number of cases showed poor response to the protocol and recurred early after resection. The presence of specific patients who have tumors which resist neoadjuvant treatment has been suggested. To improve the treatment results of PDAC, it is essential to elucidate the optimal target and resistant mechanisms for neoadjuvant therapy.

Metabolome analysis is a methodology that comprehensively measures metabolites in cells; it systematically understands the use of metabolism and cell functions and has attracted attention as a new method for post-genome research. We previously demonstrated the basic oncological mechanism in colorectal tumor by multiomics analyses (4). MYC regulates the global metabolic reprogramming of colorectal tumors (4). Recently, a number of metabolic PDAC studies have been reported. Many of them were investigated through the use of cancer cell lines or the serum of pancreatic cancer patients (5–7). In addition, few studies have examined the effect of neoadjuvant chemoradiation therapy (NACRT) of pancreatic cancer in metabolomic approaches. Therefore, the aim of this study was to investigate metabolic change in PDAC tissues that have occurred due to NACRT and the association with treatment effect and outcomes.

Methods

Patients and tissue samples

From February 2003 to August 2020, 269 patients received surgery for pancreatic cancer in Kagawa University Hospital. The optimal frozen tissue of tumor and non-neoplastic pancreas for metabolomics and genomic analysis was collected in 88 patients with informed consent during the period. The study was approved by the institutional review board of Kagawa University (Approval No. 2019-157).

Among the patients, 62 received chemoradiation therapy before pancreatectomy (NACRT group) and 26 did not receive any neoadjuvant therapies (control group). Patients in the NACRT group received the oral dose of S-1 of 60 mg/body-surface 5 days in a week and 30 Gy (2-week regimen) or 50 Gy (5-week regimen) radiation therapy (3). Patients in the control group never received any treatment before their operation. Detailed clinical data and outcomes were collected from medical records.

In the NACRT group, pathological responses were classified as poor responder (Evans grade I–IIA, $n = 43$) or good responder (Evans grade IIB–IV, $n = 18$), according to Evans classification (8). One patient could not be classified because he was unable to complete NACRT.

Tissue samples of PDAC and non-neoplastic pancreas were collected from surgical specimen immediately after resection. A 2- to 3-mm-thick slice specimen is taken from the largest circumferential surface of the PDAC tumor. Three to five random pieces of 2–3 mm^2 tissue from the slice specimen are collected in an Eppendorf tube. The tubes are immediately frozen in liquid nitrogen and preserved at −80°C for metabolome analysis.

Metabolome analysis

We performed metabolome analysis for 88 patient's tissue samples. Metabolites were measured by capillary electrophoresis-mass spectrometry (CE-MS) in the Institute for Advanced Biosciences, Keio University. Most of the metabolites related to energy metabolism, amino acid metabolism and nucleic acid metabolism that are important for cancer metabolism are ionic substances. CE-MS is suitable for measuring ionic metabolites compared with gas or liquid chromatography mass-spectrometry, nuclear magnetic resonance and most ionic substances can be directly quantitatively analyzed.

Frozen tissue samples (2–42 mg each) were completely homogenized by a cell disrupter (Shakemaster Neo; BMS, Japan) at 1500 rpm for 5–20 min, after adding 500 μl of methanol containing 20 μmol/l methionine sulfone as an internal standard. Next, 500 μl of chloroform and 200 μl of Milli-Q water were added; subsequently, the solution was centrifuged at 4600×g for 15 min at 4°C. The 300 μl upper aqueous layer was centrifugally filtered through a 5 kDa cut-off filter to remove proteins, and the solution was centrifuged at 9100×g for 3 min at 4°C. Next, the solution was centrifugal-concentrated for 1.5–4 h at 40°C, and the filtrate was lyophilized and dissolved in 50 μl of Milli-Q water containing 200 μl of 3-aminopyrrolidine and 200 μl of trimesate prior to analysis.

Cationic compounds were analyzed in the positive mode of CE-TOFMS and anionic compounds were analyzed in the positive and negative modes of CE-MS/MS, according to the methods developed by Soga et al. (9) To obtain peak information including m/z, migration time and peak area, the peaks detected by CE-TOFMS and CE-MS/MS were extracted using automatic integration software (MasterHands, Keio University, Tsuruoka, Japan and MassHunter Quantitative Analysis B.04.00, Agilent Technologies, Santa Clara, CA, USA, respectively).

Microarray

Total RNA was extracted from the frozen tissue samples of non-neoplastic and PDAC tissue in 49 patients by the Acid Guanidinium–Phenol–Chloroform method. Concentration and purity of the RNA were analyzed using the Spectrophotometer NanoDrop ND-1000 (Thermo Fisher Scientific, Inc. Waltham, MA, USA). The integrity of the RNA was analyzed using the Agilent 2100 BioAnalyzer RNA 6000 Nano Chip platform (Agilent Technologies). Fifteen pairs of non-neoplastic and PDAC tissue samples which obtained an RNA Integrity Number (RIN) >5 were judged to eligible for microarray. (NACRT group: 10 and control group: 5).

The RNA concentration ranged from 2 to 310.8 ng/μl while the mean RIN was 6.89 with a standard deviation of 0.82. RNA amplification by the Ovation Pico WTA System V2 was required because some samples had concentrations below 40 ng/μl. After RNA was qualified, 2.5 ng of total RNA was converted to cDNA, amplified and labeled with Cyanine3-labeled CTP using the SureTag Complete DNA Labeling Kit (Agilent Technologies, Santa Clara, CA). The

Table 1. Patients characteristics ($n = 88$)

	Total ($n = 88$)	Control ($n = 26$)	NACRT ($n = 62$)	P value
Age, median (range)	72 (42–90)	72 (51–90)	73 (42–87)	0.97
Gender (M/F)	42/46	14/12	28/34	0.49
CA19-9, U/ml, median (range)	88 (0.8–22 068)	95(0.8–1383)	94 (2–22 068)	0.31
PET-SUVmax median (range)	5.39 (2.6–26.22)	5.52 (2.6–19.56)	5.37 (1.04–26.22)	0.021
Histological type				
PDAC	80	19	61	0.15
Anaplastic carcinoma	3	2	1	
IPMC	2	2	0	
MiNEN	1	1	0	
Acinar cell carcinoma	1	1	0	
Squamous cell carcinoma	1	1	0	
Stage (UICC 8th), *n*				0.28
0	1	0	1	
IA	7	1	6	
IB	2	1	1	
IIA	30	10	20	
IIB	43	12	31	
III	1	0	1	
IV	3	1	2	
Unknown	1	1	0	
EVANS grade, *n*				
I	4	N/A	4	
IIA	39	N/A	39	
IIB	13	N/A	13	
III	4	N/A	4	
IV	1	N/A	1	
Unknown	1	N/A	1	

P values are based on the comparison between the control and NACRT groups. NACRT, neoadjuvant chemoradiation therapy; PDAC, pancreatic ductal adenocarcinoma; IPMC, intraductal papillary mucinous carcinoma; MiNEN, Mixed Neuroendocrine-non-neuroendocrine Neoplasm; N/A, not available.

amplified cRNA and dye incorporation were hybridized to SurePrint G3 Human GE Microarray 8 × 60 k ver. 3.0 (Agilent Technologies) 10 rpm, at 65°C for 17 h. After hybridization, arrays were washed consecutively by using the Gene Expression Wash Buffers Kit (Agilent Technologies). Fluorescence images of the hybridized arrays were generated using the SureScan Microarray Scanner, and the intensities were extracted with Agilent Feature Extraction software.

Statistical analysis

The Wilcoxon-signed rank test and Kaplan–Meier curves were performed with JMP Pro 14. Threshold value was determined using the receiver operating characteristic (ROC) curve. P values <0.05 were considered statistically significant.

Results

The backgrounds of 88 patients in this study are shown in Table 1. There was no significant difference in backgrounds between the control and NACRT groups. Eight patients are excluded from the final statistical analysis since they were not diagnosed with typical PDAC (3 for anaplastic carcinoma, 2 for IPMC, 1 for MiNEN, 1 for aciner cell carcinoma and 1 for squamous cell carcinoma) in pathological reassessment. One patient was also excluded from the analysis because only non-neoplastic tissue could be obtained.

Metabolome analysis

To analyze the metabolomic landscape, we performed CE-MS for samples of non-neoplastic and PDAC tissue in 88 patients with or without NACRT. As a result of CE-MS, more than 500 ionic metabolites were quantified. Among these, 90 metabolites that could be detected in more than 50% of the samples were statistically examined.

Figure 1 shows the heat map of metabolite levels. There appeared to be metabolic changes between PDAC and non-neoplastic tissues, and the control and NACRT groups. Specific changes were found in each group depending on whether patients received NACRT (Grade of pathological response). Score plots of primary component analysis (PCA) are shown in Supplementary Fig. 1A. Normalization by amino acid was done because several paired samples deviated from the standard. Score plots of PCA after normalization by amino acid are described in Supplementary Fig. 1B (non-neoplastic tissue vs. PDAC tissue) and Supplementary Fig. 1C (NACRT group vs. control group). There was a difference between the NACRT group and control group. Loading plots after normalization are shown in Supplementary Fig. 1D.

Major metabolite levels of PDAC and non-neoplastic pancreatic tissue are shown in Supplementary Table 1. There were various metabolomic changes between PDAC and non-neoplastic tissue. Several metabolic alterations were observed in PDAC tissue, such as the Warburg effect (10).

Metabolite level differences between the control group and NACRT group are shown in Table 2. Significant differences were found in 27 metabolites (19 decreased and 8 increased in NACRT). Comparison of potential metabolite levels between the good responder group and poor responder group is shown in Table 3. In this comparison, significant metabolic changes were observed in

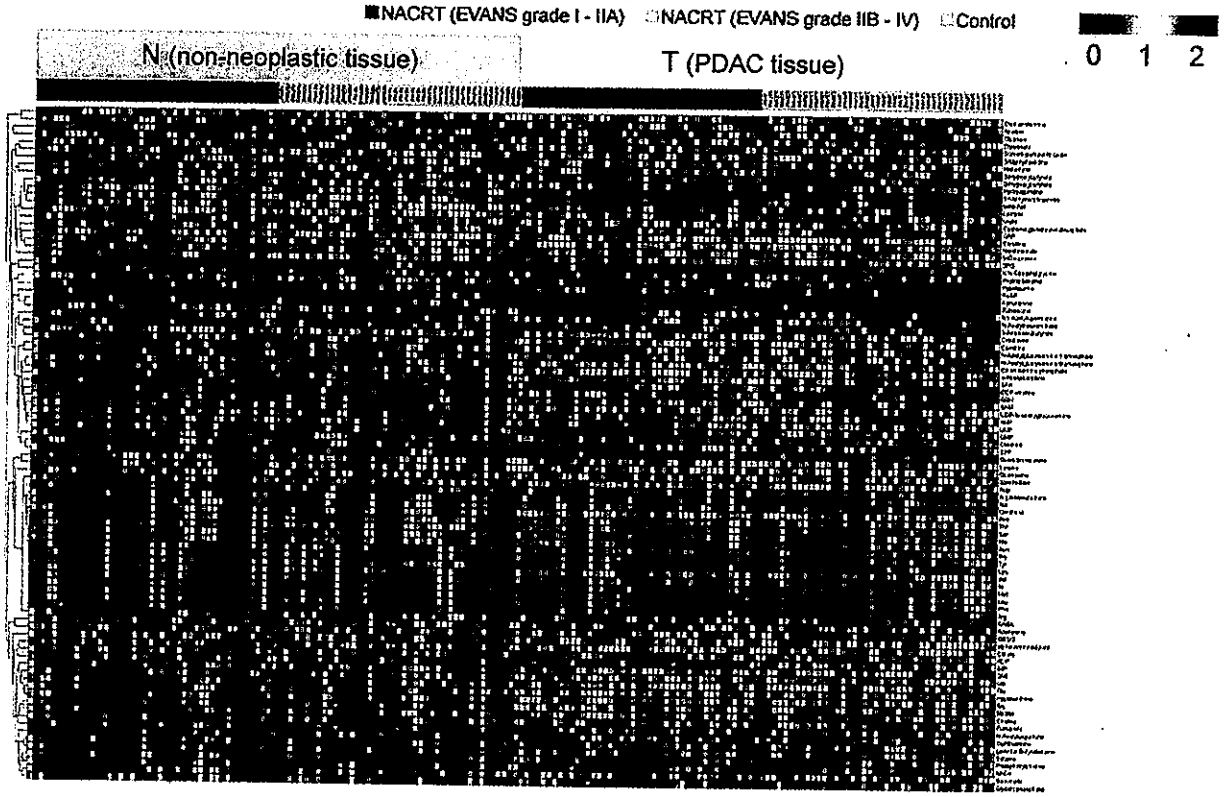

Figure 1. Metabolome analysis. Heat map of metabolite levels in paired non-neoplastic tissue and PDAC tissues obtained from 88 patients with PDAC. Each metabolite was normalized by dividing by the median of the normal tissue. Data colored in the red–white–blue scheme indicate a relatively higher, average and lower concentration, respectively. Data are horizontally arranged by groups (NACRT-EVANS grade I–IIA, NACRT-EVANS grade IIB–IV or Control) and vertically arranged by the fold change in median values of paired tumor and normal tissue. N and T indicate normal and paired tumor tissues, respectively.

eight metabolites in PDAC tissue [1-Methylnicotinamide, Carnitine, Glucose, Glutathione (red), N-acetylglucosamine 6-phosphate, N-acetylglucosamine 1-phosphate, UMP, Phosphocholine]. In addition, comparison of metabolites in PDAC tissue by treatment protocols (2-week regimen and 5-week regimen) is shown in Supplementary Table 2. No significant differences were observed in major metabolites except for 1-Methylnicotinamide.

Prognostic relevance of metabolites

Among the metabolites that indicated pathological responses, we investigated the relationship with the prognosis of patients. Threshold values for each metabolite were calculated by ROC curves, and Kaplan–Meier survival analysis for overall survival (OS) and disease-free survival (DFS) was performed. There was no significant difference in OS. Five of these metabolites [Carnitine, Glucose, Glutathione (red), Choline, Phosphocholine] were significantly associated with DFS (Table 3).

The potential metabolites for outcome, we investigated the DFS of the NACRT and control groups. Choline (≦283 nmol/mg), Phosphocholine (≦749 nmol/mg), Carnitine (≦130 nmol/mg) and Glutathione (red) (≦373 nmol/mg) levels were significantly associated with better DFS in the NACRT group. Conversely, there was no significant relationship between the levels of Phosphocholine (≦749 nmol/mg), Carnitine (≦130 nmol/mg) or Glutathione (red) (≦373 nmol/mg) levels and DFS in the control group (Figs 2 and 3). Choline (≦283 nmol/mg), which is a precursor of phosphocholine, is also associated with better DFS in both NACRT and control groups. These results suggested that the target of the NACRT effect was associated with choline metabolism in PDAC tissue.

In addition, univariate and multivariate analyses were conducted to evaluate the Choline and Phosphocholine as potential predictor for recurrence among the previously reported clinicopathologic significant factors (Supplementary Table 3). Univariate analysis showed a significant association with recurrence in PET-SUVmax (≧5.4), tumor size (≧3.0 cm), choline (≧284 nmol/mg) and phosphocholine (≧784 nmol/mg). In multivariate analysis, PET-SUVmax (≧5.4) and choline (≧284 nmol/mg) were significantly associated with recurrence.

Microarray for gene expression

Based on the results of metabolome analysis, we focused on the basic mechanism of choline metabolism on PDAC with NACRT. Figure 4 demonstrates the results of the RNA microarray related to choline metabolism. Regarding choline metabolism in cancer, it is known that choline phosphorylation pathway [Kennedy pathway (11)] is upregulated, mainly due to the overexpression of choline kinase α and choline transporters. There was no difference in the expression of choline kinase α (CHKA) between PDAC and non-neoplastic tissue. There were also no remarkable changes in gene expression related to choline synthesis and choline phosphorylation. On the other hand, choline transporters showed distinctive changes in the ratio

Table 2. Comparison of metabolite levels of PDAC tissue between NACRT and control

Metabolite mean (nmol/mg)	Control ($n = 19$)	NACRT ($n = 61$)	P value
Decreased in NACRT			
Glutathione (red)	45.78	28.9	0.0006
AMP	47.95	30.86	0.0007
SAM+	36.95	24.16	0.0025
o-Acetylcarnitine	52.9	36.37	0.0027
Phosphocholine	52.15	35.88	0.0028
UDP-N-acetylglucosamine	50.56	34.94	0.0033
GMP	35.21	23.31	0.0037
Carnitine	52.3	36.57	0.0041
ADP	46.21	32.27	0.0056
Ethanolamine phosphate	51.05	36.98	0.0092
Hypotaurine	39.47	27.98	0.01
Succinate	47.2	34.65	0.013
N1-Acetylspermidine	42.76	31.02	0.015
UMP	41.16	30.4	0.019
Creatine	49.15	37.62	0.027
Glu	49.05	37.65	0.028
Glycerophosphate	44.3	32.25	0.035
Glutathione (ox)	47.3	36.81	0.037
N-acetylaspartate	40.63	31.38	0.04
Increased in NACRT			
Diethanolamine	26.35	45.22	0.00007
Cystine	15.15	25.58	0.0066
G6P	23.94	34.74	0.021
3-Hydroxybutyrate	27.53	38.47	0.023
cis-Aconitate	15	22.22	0.035
2AB	32.45	43.18	0.037
3PG	29.58	39.61	0.039
1-Methylnicotinamide	32.75	43.08	0.043

of T/N and NACRT/control. The gene expression of several choline transporters were upregulated in PDAC tissues. Conversely, these changes were downregulated in the NACRT group. The CHTL1 (SLC5A7), major choline transporter, was slightly overexpressed in PDAC, and it was downregulated in the NACRT group. Another choline transporter CTL1-4 (SLC44A1-44A4) was overexpressed in PDAC tissue, and it was suppressed in the NACRT group. Additionally, KRAS and CDKN2A were upregulated in PDAC tissues. The levels of TP53 and SMAD4 in PDAC tissues were comparable to that of non-neoplastic tissues. Comparing the expression rates of KRAS and CDKN2A between the NACRT and control groups in PDAC tissue revealed downregulated expression.

Discussion

Metabolites reflect the end result of various changes in cancer, and many studies about cancer metabolism have been reported in recent years (12,13). Metabolomics technologies have allowed the identification of metabolite biomarkers with the promise to inform early detection of PDAC (14). On the other hand, there are few studies which have reported metabolic changes due to chemotherapy or radiation therapy (15). The present study identified new metabolic consequences of PDAC and one of the potential mechanisms of NACRT. Levels of Phosphocholine, Carnitine and Glutathione (red) were clearly associated with pathological responses and recurrence in patients with PDAC who received NACRT. It suggests that these metabolic pathways may be altered by NACRT.

Carnitine is an important metabolite in the metabolic pathway of fatty acids. Cancer cells need to produce stable energy for growth in harsh environments such as hypoxia. Like the glucose metabolism pathway, the fatty acid oxidation pathway is important for energy production in cancer cells (16). Cancer cells have a mechanism that regulates the energy production by fatty acid synthesis and fatty acid oxidation required for cell proliferation according to the environment, and this is called the carnitine system (17). In this study, the carnitine level was lower in the NACRT group than in the control group (Table 2), and it was remarkable in the good responder group (Table 3). Low carnitine levels also correlated with recurrence in the NACRT group (Fig. 3), suggesting that suppression of fatty acid metabolism may have suppressed recurrence.

Glutathione (red) removes reactive oxygen species (ROS) and protects cells from oxidative stress. Higher levels of glutathione will be easier for the cancer cells to avoid the oxidative stress and damage caused by radiation and anticancer drugs. Levels of glutathione are regulated by CD44 variant, which is an adhesion molecule expressed in cancer stem-like cells. CD44 variant (CD44v) binds to a glutamate-cystine transporter and promotes synthesis of reduced glutathione (18). In this study, higher levels of glutathione (red) in PDAC tissue were associated with recurrence in NACRT group (Fig. 3), but microarray results showed no remarkable change

Table 3. Relationship with pathological response and DFS in significant metabolites

Metabolite (Mean, nmol/mg)	Pathological response			DFS			
	Poor responder ($n = 43$)	Good responder ($n = 18$)	P value	Threshold value (nmol/mg)		Median (month)	Log-rank (P value)
1-Methylnicotinamide	33.19	24.22	0.034	20.3	> VII	15	0.057
					≤ VII	81	
Carnitine	33.45	23.61	0.022	130	> VII	11	0.022
					≤ VII	81	
Glucose	26.76	37.39	0.014	1017	> VII	81	0.049
					≤ VII	14	
Glutathione (red)	27.34	16.85	0.01	373	> VII	9	0.0047
					≤ VII	40	
N-Acetylglucosamine 6-phosphate	25.33	16.58	0.013	52.4	> VII	14	0.22
					≤ VII	28	
N-Acetylglucosamine 1-phosphate	26.12	18.46	0.045	24.7	> VII	16	0.81
					≤ VII	16	
UMP	21.23	28.88	0.034	27.6	> VII	40	0.21
					≤ VII	14	
Choline	32.38	26.11	0.1	284	> VII	11	0.0022
					≤ VII	81	
Phosphocholine	32.34	24.67	0.058	748	> VII	11	0.0086
					≤ VII	28	

Threshold value of each metabolite was calculated by ROC curves. Poor responder: Evans grade I–IIA; good responder: Evans grade IIB–IV; DFS, disease-free survival.

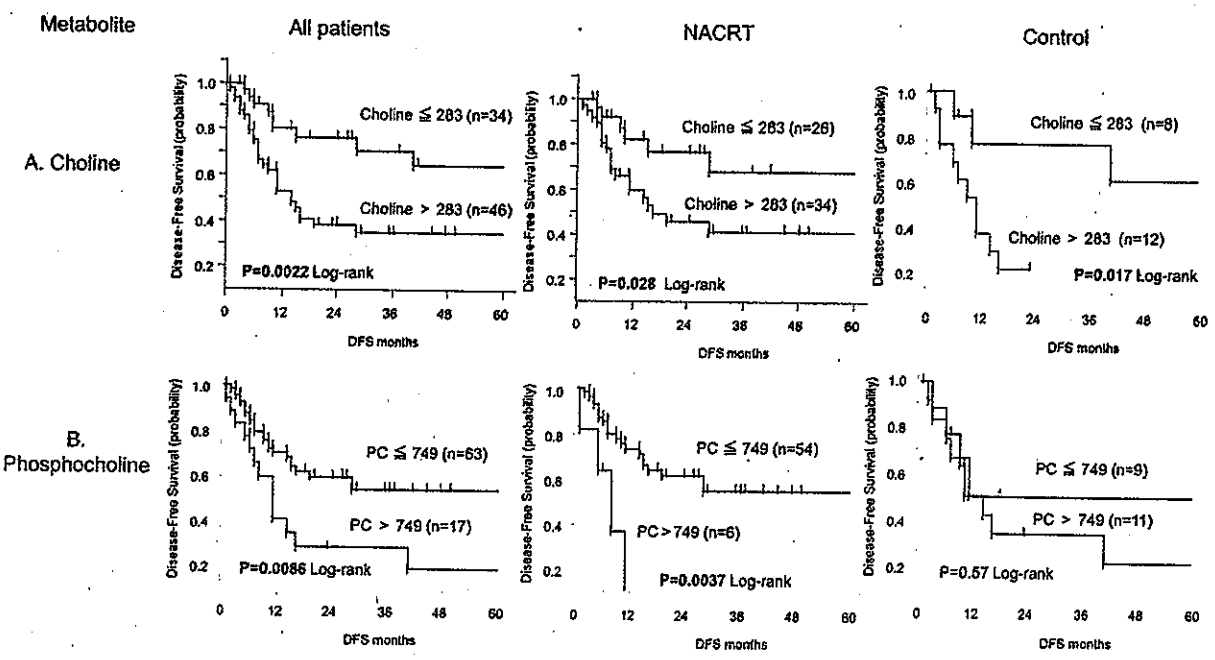

Figure 2. Kaplan–Meier curves (DFS) stratification by the level of Choline (A) and Phosphocholine (B). (A) Patients with lower levels of Choline (≤283 nmol/mg) were significantly associated with better DFS in all patients, NACRT and Control group. (B) Patients with lower levels of phosphocholine (≤749 nmol/mg) were significantly associated with better DFS in all patients and NACRT group.

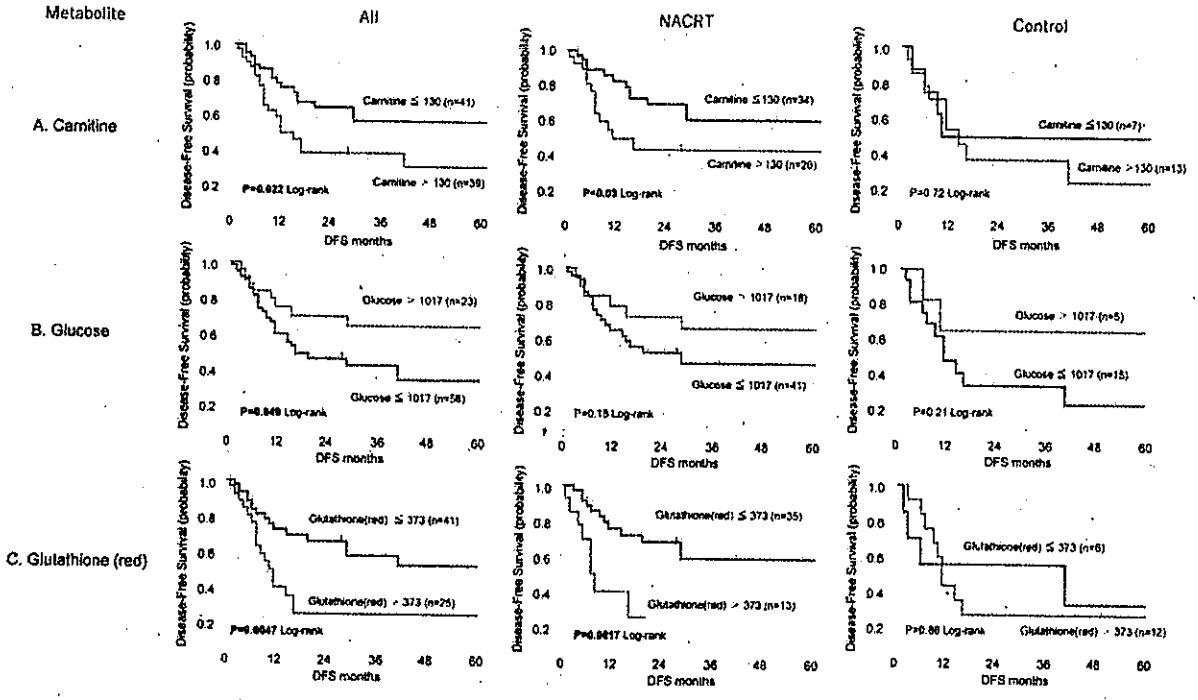

Figure 3. Kaplan–Meier curve (DFS) stratification by the level of Carnitine (A), Glucose (B) and Glutathione (red) (C). (A) Patients with lower levels of Carnitine (≤ 130 nmol/mg) were significantly associated with better DFS in all patients and NACRT group. (B) Patients with higher levels of Glucose (≥1017 nmol/mg) were associated with better DFS in all patients. (C) Patients with lower levels of Glutathione (red) (≤373 nmol/mg) were significantly associated with better DFS in all patients and NACRT group. Carnitine and Glutathione (red) had a significant association with DFS in the NACRT group.

in CD44 expression between NACRT and control group in PDAC tissues.

A study by He et al. (15) was the first to show that three metabolites, Choline, Betaine and Acetic Acid, had changed in the PDAC response to radiotherapy in a mouse xenograft model. Another study that investigated the metabolic change in patients who received preoperative chemotherapy with GEM for PDAC revealed that levels of aspartic acid were elevated in PDAC tissue. Battini et al. (19) confirmed that metabolomics profiling could predict long-term survival in 106 patients with PDAC. The elevated ethanolamine level was associated with poor survival. This study is a valuable report showing the effects of neoadjuvant therapy on PDAC. Bapio et al. (20) reported that the Kennedy pathway linked gemcitabine diphosphate choline as an important element of gemcitabine metabolic pathway in the tumors of PDAC mouse models.

Choline is indispensable for the synthesis of the major membrane phospholipid phosphatidylcholine. Previous studies have demonstrated elevation in choline level and choline phospholipid metabolism in cancer cells (21). There are three main pathways for choline metabolism. Choline methylation synthesizes betaine, which acts as the methyl donor, and acetylation of choline produces acetylcholine, a precursor of a neurotransmitter (22). The choline phosphorylation pathway is called the Kennedy pathway, which synthesizes the major membrane phospholipids phosphatidylcholine and sphingomyelin. Choline uptake and phosphorylation are activated in cancer and play an important role for tumor growth (23,24). Choline PET is used as a clinically diagnostic tool for cancer patients utilizing the property (25). Activation of the Kennedy pathway was reported in PDAC cell lines with overexpression of choline kinase-α and choline transporters (26). Choline kinase α and choline transporters are attracting attention as therapeutic targets, and thus, inhibitors are being developed.

Metabolome analysis in this study showed significant changes in choline metabolism in the NACRT group, especially in the good response group. Choline and phosphocholine levels in tumors are increased by enhancing the Kennedy pathway (11). Choline and phosphocholine levels were significantly lower in the NACRT group than in the control group in PDAC tissue. These levels were especially lower in the good response group, suggesting that NACRT may have suppressed the Kennedy pathway. In comparison with PDAC and non-neoplastic tissues, choline and phosphocholine levels were lower in tumor tissues (Supplementary Table 1). Suppression of the Kennedy pathway in the NACRT group could be responsible for lower levels of choline and phosphocholine in PDAC tissue. The Warburg effect is well known as major metabolic change in cancer, in which glycolysis is enhanced even when oxygen demand is sufficient (27). The common feature of this altered metabolism is increased glucose uptake and fermentation of glucose to lactate (10). In this study, a high level of lactate concentration was observed, as in previous reports, and NACRT did not show any inhibitory effect.

We investigated the relationship between metabolite levels and prognosis to confirm whether metabolic changes reflected treatment effects. There were several metabolite levels in PDAC tissues, which had significant relationships with DFS. There was no significant difference in OS in each possible metabolite. It may reflect that most patients received postoperative powerful treatment including FOLFIRINOX and/or Gemcitabine plus *nab*-paclitaxel (GnP) after recurrence. The DFS is thought to be reliable evidence of the therapeutic effect of NACRT. Interestingly, phosphocholine was associated

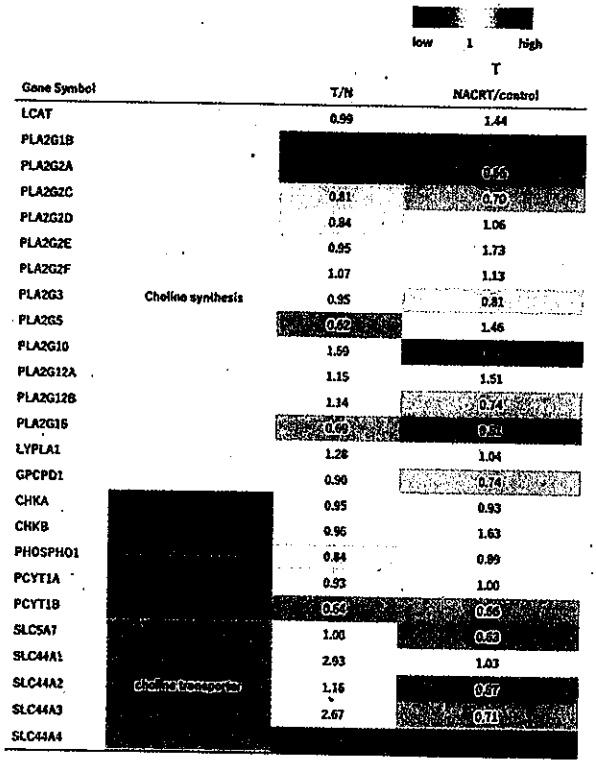

Figure 4. Microarray analysis for genes involved in choline metabolism (N, non-neoplastic tissue; T, PDAC). T/N: Ratio of gene expression between tumor and non-neoplastic in 15 patients. NACRT/control: Ratio between NACRT group ($n = 10$) and control group ($n = 5$) was calculated in each PDAC tissue. Choline transporters were overexpressed in PDAC tissue. Expression of choline transporters were suppressed in NACRT group.

with recurrence-free survival in the NACRT group. This result suggests that choline metabolism is one of the key components for the effect of NACRT in PDAC.

Surprisingly, the higher level of choline in the tumor was an independent significant predictor of recurrence among previously reported significant clinicopathologic factors (Supplementary Table 3). The results suggested that tumor choline metabolism is one of the key pathways involved in recurrence and also should be a potential target of development of new markers for predicting recurrence of pancreatic cancer.

The microarray focused on genes related to choline metabolism based on the results of metabolome analysis and survival curves in the present study. In the Kennedy pathway, choline kinase and the choline transporter have important roles. Eight types of choline transporters were reported (28). Among these, high-affinity choline transporter 1 (CHT1/SLC5A7) and choline transporter-like proteins CTLs/SLC44 family (CTL1-5/SLC44A1-5) had a main role of choline intake. Additionally, increased CHT1, CTL1 and CTL2 expression levels have been reported in PDAC (26).

In this study, overexpression of choline kinases was not confirmed in PDAC tissue from the microarray. Regarding the transporters, expression levels of all transporters were increased in PCAC versus non-neoplastic tissues. Comparing the NACRT and control, we observed that the transporter expression in the NACRT group was clearly decreased. This suggested that the decreased levels of phosphocholine and choline might be related to transporter expression rather than choline kinase. CTL4 (SLC44A4) was the most highly expressed transporter. CTL4 does not have the function of choline transport, but it plays a role in transporting thiamine pyrophosphate. Thiamine pyrophosphate has important role in ATP production in the TCA cycle and the pentose phosphate cycle, fatty acid and nucleic acid production, and glucose metabolism. CTL4 is highly expressed in prostate cancer and colon cancer, and therapeutic agents targeting CTL4 are being developed (29). CTL4 has no choline transport ability; thus, it might not be deeply involved in the change of choline metabolism in this study.

This study suggested that NACRT may affect choline metabolism, and lower levels of choline and phosphocholine correlated with the low recurrence rate in the NACRT group. Radiation and the anti-cancer drug 5-FU for sensitizing action were used in combination in the study. The mechanism and relationship of each treatment components remain unclear. Changes in choline levels with radiation have been reported in studies in mice (15). Although there has never been a report that 5-FU has an effect on choline metabolism, a study has reported that a combination with a choline kinase inhibitor is useful in colorectal cancer (30). The results suggest that therapeutics that target choline metabolism may also be effective in pancreatic cancer.

Several limitations of the study should be mentioned. First, the metabolic data before the preoperative treatment could not be obtained in this study. It may be ideal to compare tissues before and after treatment in the same patient. It is difficult to secure enough tissue from the preoperative biopsy to perform metabolome analysis. It is also unclear whether metabolic changes in tissues can detected in the serum as well. As serum can be collected safely before and after NACRT, the changes in serum choline levels before and after NACRT are an attractive subject in follow-up research. The second limitation is that the number of patients in the study may not be enough to draw firm conclusions. Since NACRT has not been standardized in clinical practice yet, collecting a large number of sufficient samples in the same protocols is difficult at this time. We hope that the proposed metabolomic consequence of neoadjuvant treatment for PDAC will be verified by future large-scale research. Third, the NACRT regimen in the study is not a current standard protocol such as Gemcitabine plus S-1 therapy. It is unclear whether the metabolic changes observed in this study observed in other regimens as well. We hope that future studies will be promoted based on the results of this study. Lastly, influence of the ROS in the sample should be considered, as altered metabolites and gene expression are associated with redox.

In conclusion, the present study identifies new metabolic consequences and potential target of NACRT for PDAC. Choline metabolism is clearly associated with pathological responses and recurrence in patients with PDAC who received NACRT. NACRT may improve the prognosis of patients with PDAC through the alteration of choline metabolism. Choline metabolism might be a potential key target and biomarker of neoadjuvant treatment for PDAC.

Supplementary material

Supplementary material is available at *Japanese Journal of Clinical Oncology* online.

Acknowledgements

We would like to thank Editage (www.editage.com) for English language editing.

Funding

Supported by a Grant-in-Aid for Scientific Research (18K07298) from the Ministry of Education, Science and Culture of Japan.

Conflict of interest statement

The authors have no financial conflicts of interest related to this work.

References

1. Uesaka K, Boku N, Fukutomi A, et al. Adjuvant chemotherapy of S-1 versus gemcitabine for resected pancreatic cancer: a phase 3, open-label, randomised, non-inferiority trial (JASPAC 01). *Lancet* 2016;388:248–57.
2. Jang JY, Han Y, Lee H, et al. Oncological benefits of neoadjuvant chemoradiation with gemcitabine versus upfront surgery in patients with borderline resectable pancreatic cancer: a prospective, randomized, open-label, multicenter phase 2/3 trial. *Ann Surg* 2018;268:215–22.
3. Okano K, Suto H, Oshima M, et al. A prospective phase II trial of neoadjuvant S-1 with concurrent hypofractionated radiotherapy in patients with resectable and borderline resectable pancreatic ductal adenocarcinoma. *Ann Surg Oncol* 2017;24:2777–84.
4. Satoh K, Yachida S, Sugimoto M, et al. Global metabolic reprogramming of colorectal cancer occurs at adenoma stage and is induced by MYC. *Proc Natl Acad Sci U S A* 2017;114:E7697–706.
5. Fujita M, Imadome K, Imai T. Metabolic characterization of invaded cells of the pancreatic cancer cell line, PANC-1. *Cancer Sci* 2017;108:961–71.
6. Itoi T, Sugimoto M, Umeda J, et al. Serum metabolomic profiles for human pancreatic cancer discrimination. *Int J Mol Sci* 2017;18:767.
7. Wen S, Zhan B, Feng J, et al. Non-invasively predicting differentiation of pancreatic cancer through comparative serum metabonomic profiling. *BMC Cancer* 2017;17:708.
8. Evans DB, Rich TA, Byrd DR, et al. Preoperative chemoradiation and pancreaticoduodenectomy for adenocarcinoma of the pancreas. *Arch Surg* 1992;127:1335–9.
9. Soga T, Baran R, Suematsu M, et al. Differential metabolomics reveals ophthalmic acid as an oxidative stress biomarker indicating hepatic glutathione consumption. *J Biol Chem* 2006;281:16768–76.
10. Liberti MV, Locasale JW. The Warburg effect: how does it benefit cancer cells? *Trends Biochem Sci* 2016;41:211–8.
11. McMaster CR. From yeast to humans - roles of the Kennedy pathway for phosphatidylcholine synthesis. *FEBS Lett* 2018;592:1256–72.
12. DeBerardinis RJ, Chandel NS. Fundamentals of cancer metabolism. *Sci Adv* 2016;2:e1600200.
13. Hay N. Reprogramming glucose metabolism in cancer: can it be exploited for cancer therapy? *Nat Rev Cancer* 2016;16:635–49.
14. Ritchie SA, Akita H, Takemasa I, et al. Metabolic system alterations in pancreatic cancer patient serum: potential for early detection. *BMC Cancer* 2013;13:416.
15. He XH, Li WT, Gu YJ, et al. Metabonomic studies of pancreatic cancer response to radiotherapy in a mouse xenograft model using magnetic resonance spectroscopy and principal components analysis. *World J Gastroenterol* 2013;19:4200–8.
16. Qu Q, Zeng F, Liu X, Wang QJ, Deng F. Fatty acid oxidation and carnitine palmitoyltransferase I: emerging therapeutic targets in cancer. *Cell Death Dis* 2016;7:e2226.
17. Melone MAB, Valentino A, Margarucci S, Galderisi U, Giordano A, Peluso G. The carnitine system and cancer metabolic plasticity. *Cell Death Dis* 2018;9:228.
18. Ishimoto T, Nagano O, Yae T, et al. CD44 variant regulates redox status in cancer cells by stabilizing the xCT subunit of system xc(−) and thereby promotes tumor growth. *Cancer Cell* 2011;19:387–400.
19. Battini S, Faitot F, Imperiale A, et al. Metabolomics approaches in pancreatic adenocarcinoma: tumor metabolism profiling predicts clinical outcome of patients. *BMC Med* 2017;15:56.
20. Bapiro TE, Frese KK, Courtin A, et al. Gemcitabine diphosphate choline is a major metabolite linked to the Kennedy pathway in pancreatic cancer models in vivo. *Br J Cancer* 2014;111:318–25.
21. Eliyahu G, Kreizman T, Degani H. Phosphocholine as a biomarker of breast cancer: molecular and biochemical studies. *Int J Cancer* 2007;120:1721–30.
22. Michel V, Yuan Z, Ramsubir S, Bakovic M. Choline transport for phospholipid synthesis. *Exp Biol Med (Maywood)* 2006;231:490–504.
23. Glunde K, Bhujwalla ZM, Ronen SM. Choline metabolism in malignant transformation. *Nat Rev Cancer* 2011;11:835–48.
24. Glunde K, Serkova NJ. Therapeutic targets and biomarkers identified in cancer choline phospholipid metabolism. *Pharmacogenomics* 2006;7:1109–23.
25. Hodolič M. Imaging of prostate cancer using (18)F-choline PET/computed tomography. *PET Clin* 2017;12:173–84.
26. Pener MF, Shah T, Bharti S, et al. Metabolic imaging of pancreatic ductal adenocarcinoma detects altered choline metabolism. *Clin Cancer Res* 2015;21:386–95.
27. Warburg O. On the origin of cancer cells. *Science (New York, NY)* 1956;123:309–14.
28. Inazu M. Choline transporter-like proteins CTLs/SLC44 family as a novel molecular target for cancer therapy. *Biopharm Drug Dispos* 2014;35:431–49.
29. Mattie M, Raitano A, Morrison K, et al. The discovery and preclinical development of ASG-5ME, an antibody-drug conjugate targeting SLC44A4-positive epithelial tumors including pancreatic and prostate cancer. *Mol Cancer Ther* 2016;15:2679–87.
30. de la Cueva A, Ramirez de Molina A, Alvarez-Ayerza N, et al. Combined 5-FU and ChoKalpha inhibitors as a new alternative therapy of colorectal cancer: evidence in human tumor-derived cell lines and mouse xenografts. *PLoS One* 2013;8:e64961.